Supporting Information

Tailoring the SWIR emission of gold nanoclusters by surface ligand rigidification and their application in 3D bioimaging

Xavier Le Guével[a*†], K. David Wegner[b†], Christian Würth[b], Vladimir A. Baulin[c], B. Musnier[a], V. Josserand[a], U. Resch-Genger[b], and Jean-luc Coll[a]

Synthesis of gold nanoclusters (Au NCs). All products were purchased from Sigma-Aldrich (France) and we used deionized water. AuMHA/TDT was prepared in a similar protocol reported previously[1]. Briefly, 500 µL of $HAuCl4.3H_20$ (20mM) was added to 4.8 mL of water followed by 4 mL of the thiolated ligand mixture mercaptohexanoic acid (MHA, 5 mM; 2mL) / tetra(ethyleneglycol) dithiol (TDT, 5 mM, 2mL) changing color from yellowish to slightly pale cloudy. After 1 min, 500 µL of NaOH (1M) was added dropwise leading to almost colorless sols. After 5 min, 150 µL $NaBH_4$ (20 mM in 0.2 M NaOH) was introduced dropwise under mild stirring at 350rpm for 8 hours. Purification of the AuMHA/TDT on 3 kDa cut-off filter column (Amicon) were repeated 3 times to stop the reaction and sols were kept stored in the fridge before use. Synthesis yield was determined optically on a spectrophotometer by the consumption of gold salt[2] to produce Au NCs and estimated around 90%.

Composite. AuMHA/TDT embedded in PDMS was prepared using a protocol described elsewhere[3].

Microscopy. Metal core sizes were determined by high resolution transmission electron microscopy with an 200 kV monochromated TEM using dispersed Au NCs on ultra-fine carbon films.

Optical characterization.

Absorption spectra of diluted AuNC samples were recorded on an Safas Monaco SP2000 UV-vis spectrophotometer between 350 and 1100 nm. Steady-state photoluminescence spectra were measured from 600 – 1750 nm with a calibrated FSP 920 (Edinburgh Instruments, Edinburgh, United Kingdom) spectrofluorometer equipped with a nitrogen-cooled PMT R5509P. Time-resolved measurements were performed in the wavelength region of 300 – 1100 nm using a FLS 920 (Edinburgh Instruments, Edinburgh, United Kingdom) lifetime spectrofluorometer equipped with an EPL-510 (Edinburgh Instruments, Edinburgh, United

Kingdom) picosecond pulsed diode laser (excitation wavelength of 510±10 nm; power of 5mW) and a fast PMT R2658P from Hamamatsu , respectively. The PL decays were fitted with a multi-exponential model, see Eq. (1)

$$I(t) = \sum_n a_n e^{(-t/\tau_n - \frac{t}{\tau_n})} \quad (1)$$

where a_n are the amplitudes and τ_n the lifetimes of the respective decaying species. These data were calculated with a reconvolution fitting procedure using the FLS-920 spectrometer software. The fit quality was evaluated from the corresponding χ^2 values. The average lifetimes were calculated as an intensity-weighted average, see Eq. (2)

$$<\tau>_{int} = \frac{\sum_n A_n \tau_n^2}{\sum_n A_n \tau_n} \quad (2)$$

where, τ_n are the lifetimes of each component and A_n the corresponding relative fractional amplitudes.

In vivo SWIR imaging was performed on a NMRI nude female mice perfused with AuMHA/TDT (5 mg Au/mL) using a Nirvana 640ST (Princeton) and a laser excitation at 808 nm (120 mW/cm^2). Images were taken with 25mm lens (Navitar) with n.a= 4.8 using a long pass filter at 1319 nm (Semrock) and recorded at 250 ms acquisition time. A tilt support (Thorlabs) enabled to take pictures from -45° to +45° every 0.5° step.

All animal experiments followed the institutional guidelines of the European Community (EU Directive 2010/63/EU) for the use of experimental animals and were approved by an ethic committee (Cometh38 Grenoble, France) and the French Ministry of Higher Education and Research under the reference: APAFIS#8854-20 17031314338357 v1.

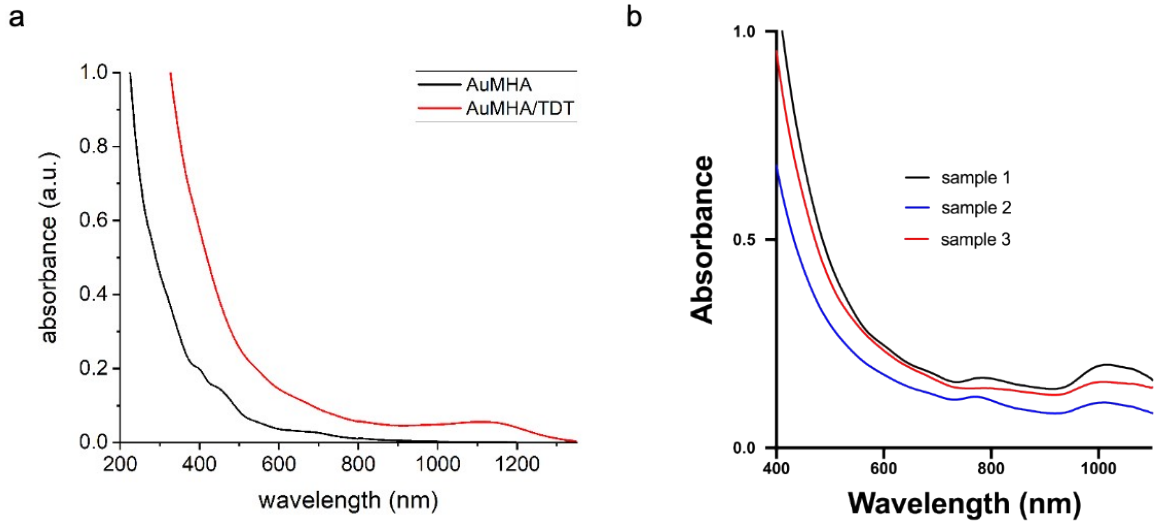

Figure S1. Absorbance spectra of (a) AuMHA and AuMHA/TDT dispersed in water, (b) AuMHA/TDT dispersed in water and prepared in different synthesis.

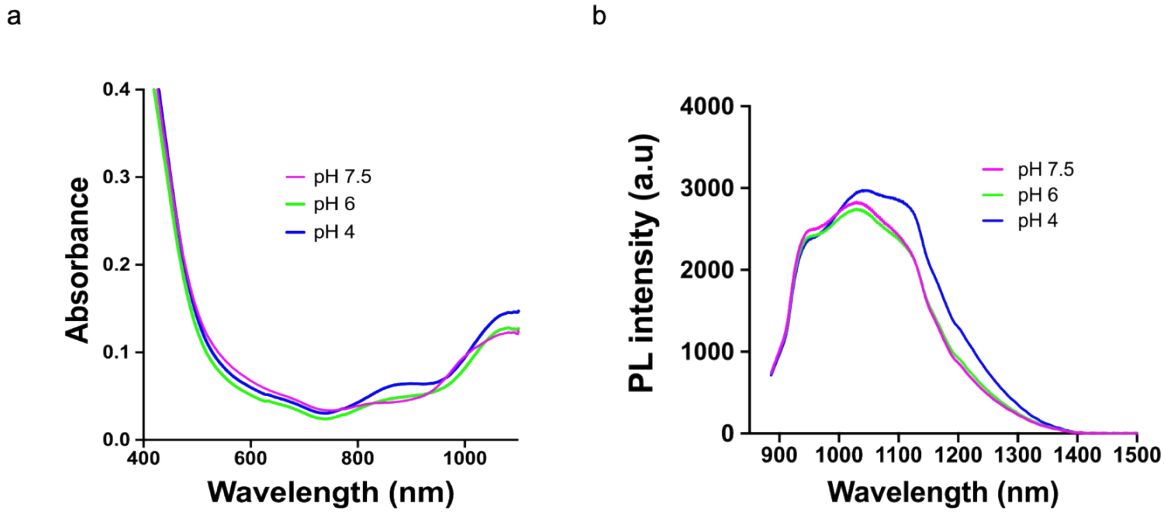

Figure S2. (a) Absorbance spectra and (b) PL spectra ($\lambda_{exc.}$ 808 nm) of AuMHA/TDT at different pH.

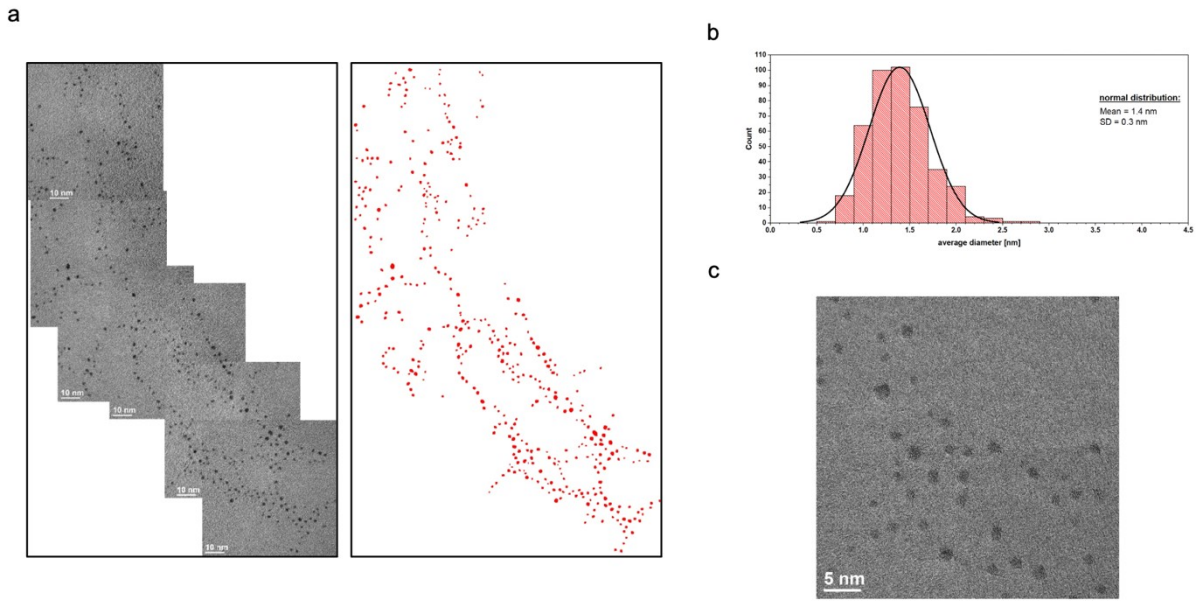

Figure S3. High resolution transmission electron microscopy (HRTEM) of AuMHA/TDT dispersed in water showing a long-distance organisation (a) of narrow particle size distribution (b) with semi-crystalline structure (c). Size distribution was estimated with ~ 400 single gold nanoclusters from TEM images.

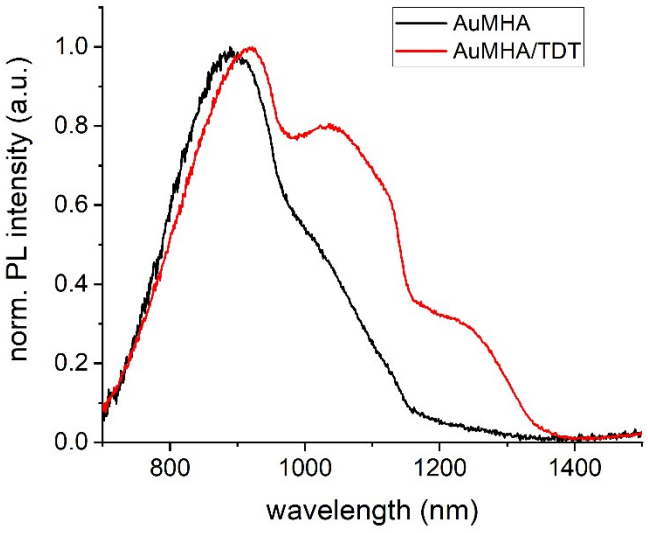

Figure S4. Normalized PL spectra of AuMHA and AuMHA/TDT excited at 400 nm.

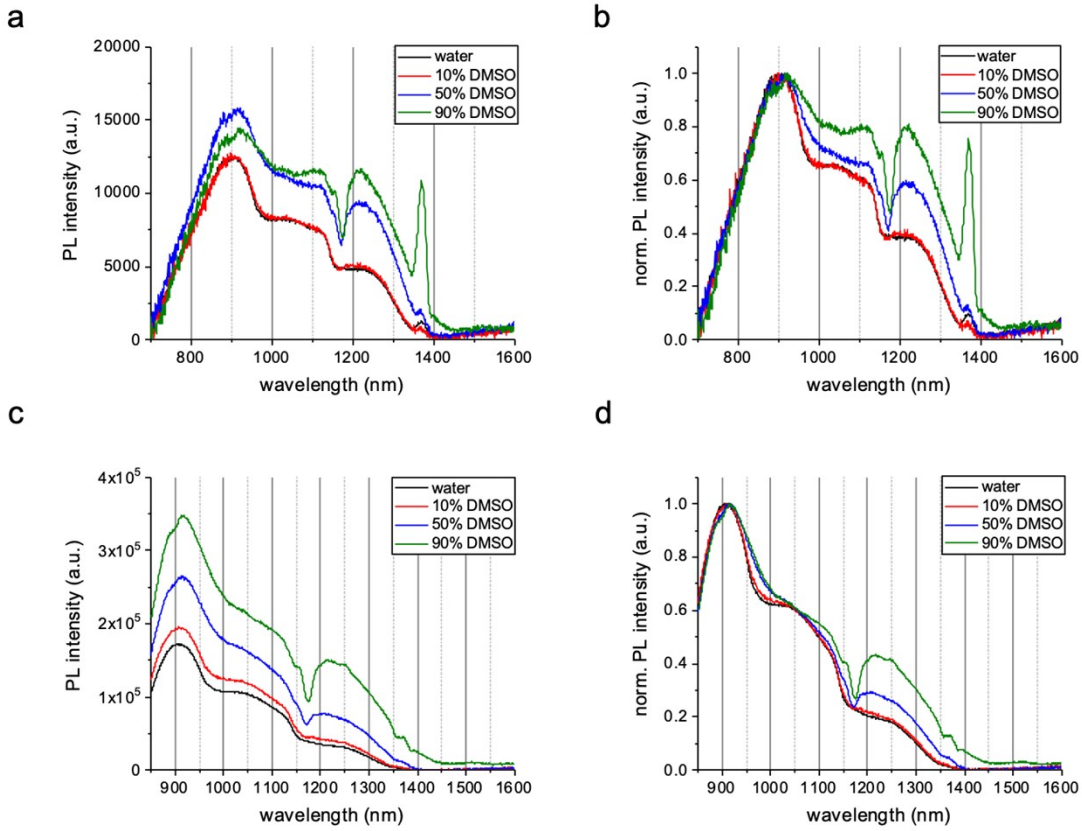

Figure S5. (a) PL spectra and (b) normalised PL spectra at λ= 920 nm of AuMHA/TDT dispersed in mixture DMSO/water ($\lambda_{exc.}$ 680 nm). The peak at 1360 nm is caused by the second harmonic generation of the excitation light. (c) PL spectra and (d) normalised PL spectra at λ= 920 nm of AuMHA/TDT dispersed in mixture DMSO/water ($\lambda_{exc.}$ 830 nm). For increasing DMSO concentration the solvent absorbance causes a dip around 1150 nm.

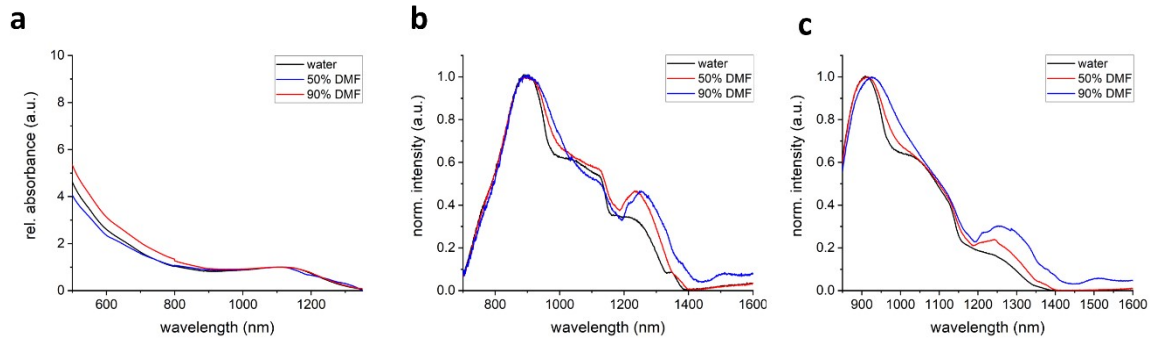

Figure S6. (a) Absorbance spectra of AuMHA/TDT dispersed in DMF/water mixtures. PL spectra of AuMHA/TDT using excitation wavelengths at 680 nm (b) and at 830 nm (c) were measured in different DMF/water mixtures.

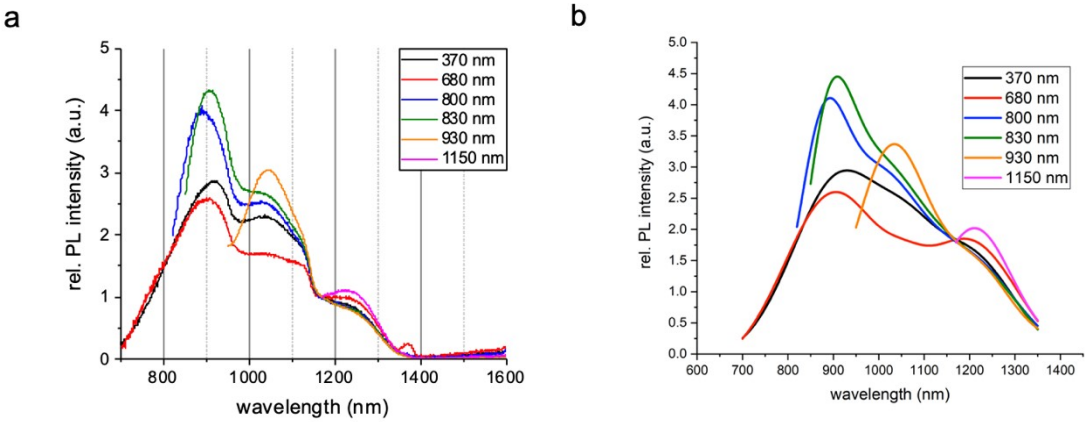

Figure S7. PL spectra before (a) and after (b) water absorbance correction of AuMHA/TDT measured at different excitation wavelength.

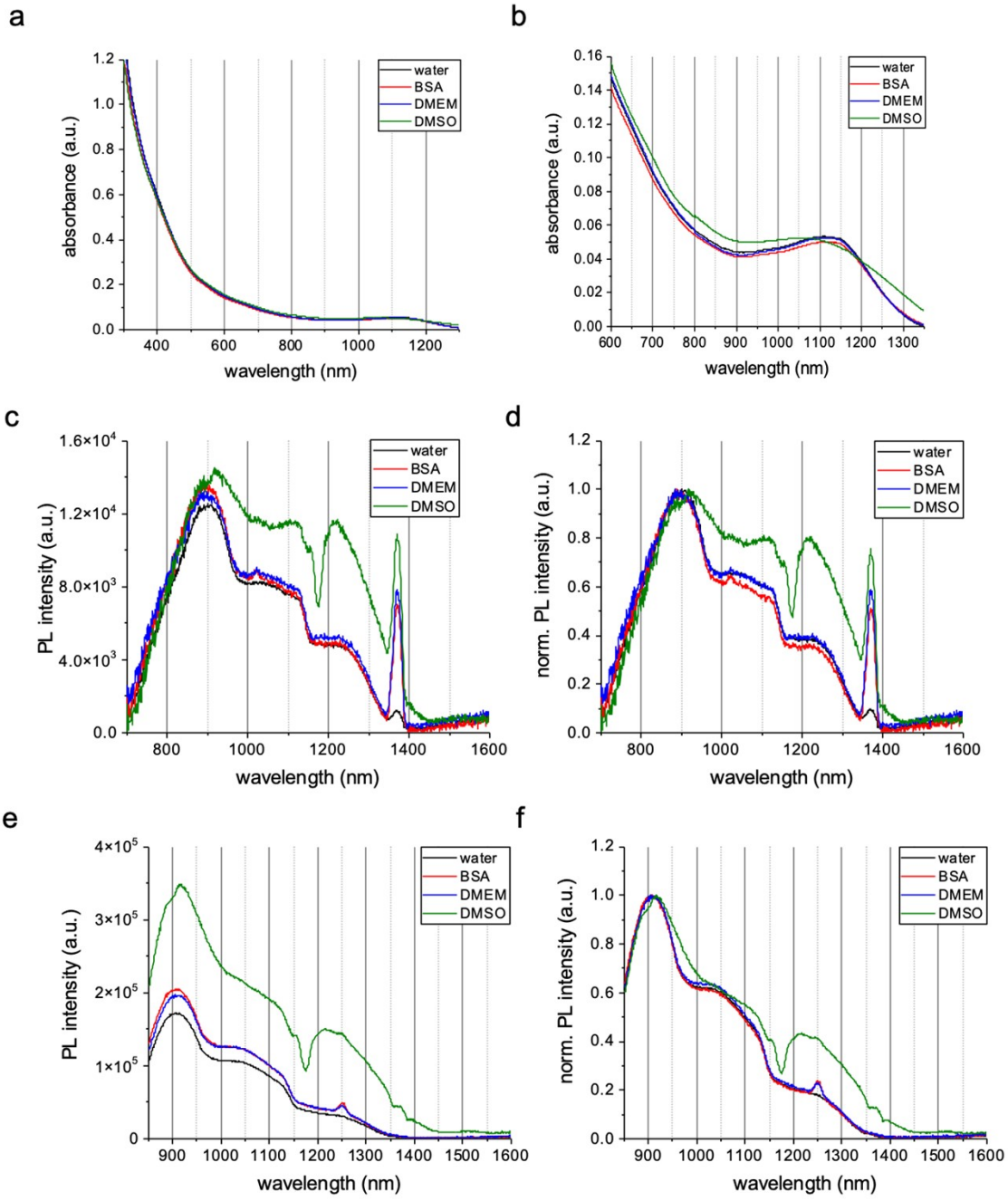

Figure S8. (a,b) Absorbance spectra of AuMHA/TDT dispersed in different media. (c) PL spectra and (d) normalised PL spectra at λ= 920 nm of AuMHA/TDT dispersed in different media ($\lambda_{exc.}$ 680 nm). The peak at 1360 nm is caused by the second harmonic generation of the excitation wavelength. (e) PL spectra and (f) normalised PL spectra at λ= 920 nm of AuMHA/TDT dispersed in different media ($\lambda_{exc.}$ 830 nm).

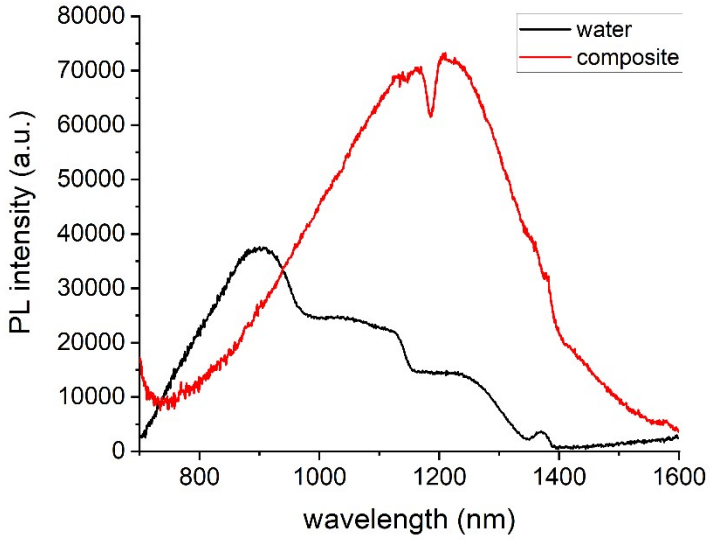

Figure S9. PL spectra of AuMHA/TDT dispersed in water and in embedded in the PDMS composite. ($\lambda_{exc.}$ = 680 nm)

Table S1. Decay time analysis of AuNCs in solution and in composite and the calculated intensity weighted average decay time.

	A_1	τ_1 (ns)	A_2	τ_2 (ns)	A_3	τ_3 (ns)	$\langle\tau\rangle_{int}$ (ns)
solution	2201	100.8	2687	432.3	432	1603.0	**787**
composite	1732	30.4	1049	138.5	238	571.8	**298**

References

[1] B. Musnier, K.D. Wegner, C. Comby-Zerbino, V. Trouillet, M. Jourdan, I. Hausler, R. Antoine, J.L. Coll, U. Resch-Genger, X. Le Guevel, Nanoscale, 11 (2019) 12092-12096.
[2] S.R. King, J. Massicot, A.M. McDonagh, Metals, 5 (2015) 1454-1461.
[3] B. Musnier, M. Henry, J. Vollaire, J.-L. Coll, Y. Usson, V. Josserand, X. Le Guével, Journal of Biophotonics, n/a (2020) e202000345.